Ménard, Cécile B.; Essery, Richard; Pomeroy, John; Marsh, Philip; Clark, Douglas B. 2014. **A shrub bending model to calculate the albedo of shrub-tundra**. *Hydrological Processes* 28 (2). 341-351. 10.1002/hyp.9582

A shrub bending model to calculate the albedo of shrub-tundra

Cécile B. Ménard[1], Richard Essery[2], John Pomeroy[3], Philip Marsh[4], and Douglas B. Clark[5]

[1]Finnish Meteorological Institute, Arctic Research Centre, Helsinki, Finland
[2]School of Geosciences, University of Edinburgh, Edinburgh, UK
[3]Centre for Hydrology, University of Saskatchewan, Saskatoon, Canada
[4]National Hydrology Research Centre, Environment Canada, Saskatoon, Canada
[5]Centre for Ecology and Hydrology, Wallingford, UK

Abstract

At high latitudes, the albedo and energy budget of shrub-tundra landscapes is determined by the relationship between the fractional snow cover and the fraction of vegetation protruding above the snowpack. The exposed vegetation fraction is affected by the bending and / or burial of shrubs in winter and their spring up during melt. Little is known about the meteorological conditions and snowpack and shrub properties required to cause bending, and few quantitative measurements of bending processes exist. Here, a model combining the few, mostly qualitative, observations available with a biomechanical model representing branches as cantilevers is proposed to provide a first approximation of bending mechanisms. The exposed vegetation fraction is then calculated using structural parameters of shrubs measured at two sites in Canada: the Granger Basin in the Yukon Territory and Trail Valley Creek in the Northwest Territories. The exposed vegetation fraction is in turn used to calculate albedo, which is evaluated against measurements at the two sites. The model considerably improves modelled albedo compared to a model which only buries but does not bend shrubs at TVC, where shrubs become completely buried. However, the model overestimates albedo at GB where only a few shrubs get buried. The bending model is then used to calculate a compression factor for use in a simple parametrization of the exposed vegetation fraction proposed by previous investigators. The parametrization, which is simpler and computationally less expensive than the full model, is evaluated and found to perform well. Despite the need for further developments, the model provides a first approximation of bending processes and contributes to the identification of measurements that are needed in order to improve the model and our understanding of the bending of shrubs.

1 Introduction

Increases in shrub biomass and abundance at northern latitudes have garnered much attention over recent years. This shift in land surface cover from open-tundra dominated by snow cover in winter to shrub-tundra with shrubs protruding above the snowpack is expected to decrease albedos and increase surface

temperatures (Chapin III et al., 2005). This "shrubification"-induced decrease in albedo may be partially offset by shrubs bending under the weight of snow and becoming buried in the snowpack. Previous studies (e.g. Sturm et al., 2005, Pomeroy et al., 2006, Marsh et al., 2010) have reported that tall (> 1.5 m) shrub sites and open tundra can have similar energy balances in winter because shrub branches bend and then are buried under the snow, springing up again as the snow melts. Shrub mechanics therefore have implications for both winter and spring energy budgets. Sturm et al. (2005b) calculated that differences in absorbed solar radiation from October to March between shrub-free tundra and shrubland can be of the order of 69 to 75% despite the limited sunlight available at high latitudes. Loranty et al. (2011) found that differences in albedo between tundra and shrub-tundra can lead to differences in net radiation greater than 50 W m^{-2} during melt. Tall shrubs also promote turbulent exchanges of heat between the surface and the atmosphere because they increase the roughness of the surface. As a consequence, recent studies have identified the representation of shrub bending and burying processes as critical to the modelling of high latitude energy balances (Sturm et al., 2005a; Bewley et al., 2010).

Although bending is a common evolutionary trait amongst shrubs in cold environments (Johnson, 1987; Beismann et al., 2000), the study of this mechanical process for hydrometeorological applications is still in its infancy and little is known about the environmental conditions necessary to cause bending. In addition, because of the non-systematic bending of branches and the destructive nature of measurements, most hypotheses on shrub bending and spring-up processes have been based on qualitative observations. These hypotheses include:

1. Bending occurs at near-freezing temperatures when snow is wet and adheres to branches (Sturm et al., 2005b, Pomeroy et al., 2006).

2. Bending occurs during high winds which contribute to the laying-down of shrubs (Sturm et al., 2005b, Pomeroy et al., 2006).

3. Bending can occur in less than one day (Sturm et al., 2005a).

4. Stem diameter is the main factor and species secondary (Sturm et al., 2005b).

5. Burial is not systematic and does not occur every year (Pomeroy et al., 2006, Marsh et al., 2010).

6. Tall willow and birch are more susceptible to bending than alder shrubs, even though any shrub can become buried (Pomeroy et al., 2006).

7. Shrub spring-up is associated with wet snow metamorphism and changing elasticity due to branch warming (Pomeroy et al., 2006).

The nature of bending makes the collection of quantitative data difficult. The non-systematic bending of shrubs makes it logistically difficult to predict where and when data may be best collected. With regards to spring-up, getting a better understanding of the relationship between snow-grain bond weakening, snow metamorphism and elasticity involves the use of destructive methods which may counteract the knowledge gained. As a consequence, measurements of albedo, which are non-destructive and easy to collect, have often

been used as a proxy to understand shrub bending and spring-up behaviour (Sturm et al., 2005; Liston and Hiemstra, 2011; Endrizzi and Marsh, 2011).

Endrizzi and Marsh (2010) and Liston and Hiemstra (2011) have tested models with separate energy balances for snow and exposed vegetation. For use in earth system models, Liston and Hiemstra (2011) proposed a parametrization

$$F_v = F_{v0} \max \left[0, 1 - \left(\frac{S_d}{bh_c} \right)^a \right] \tag{1}$$

for exposed vegetation fraction, where F_{v0} is the snow-free vegetation fraction, S_d is snow depth, h_c is canopy height and a is a shape factor equal to 1 for parabola-shaped shrubs or 2 for hemisphere-shaped shrubs. Following Sturm et al. (2005a), b is a compression factor which remains close to 1 for stiff shrubs that remain erect but decreases as snow depth increases for flexible shrubs that bend under their loads of intercepted snow. Although Sturm et al. (2005a) and Liston and Hiemstra (2011) discuss how different values of b lead to different albedo and energy balance regimes, they do not propose methods to calculate it. This paper builds on these studies and proposes a mechanistic shrub bending model driven by meteorological data to calculate exposed vegetation fraction during cycles of snow accumulation and ablation. The vegetation fraction is then used to calculate albedo, which is evaluated against observations at two sites covering five winters. The model is then used to calculate b for a parametrization of the exposed vegetation fraction and albedo of shrub-tundra. A list of parameters and variables used in the model can be found in Table 6.

2 Description of the Shrub Bending Model

2.1 Albedo calculation

The effective albedo of a landscape with exposed vegetation fraction F_v, snow cover fraction F_s and exposed ground fraction $1 - F_s$ is calculated here as

$$\alpha = F_s(1 - F_v)\alpha_s + (1 - F_v)(1 - F_s)\alpha_g + F_v\alpha_v \tag{2}$$

where α_g and α_v are the ground and vegetation albedo respectively. Snow albedo α_s is assumed to decrease with time following Verseghy (1991) such that

$$\alpha_s(t + \Delta t) = [\alpha_s(t) - \alpha_{s(min)}] \exp \left(\frac{-0.01\Delta t}{3600} \right) + \alpha_{s(min)} \tag{3}$$

where Δt is the length of the model timestep in seconds and $\alpha_{s(min)}$ is the lower limit for snow albedo, taken to be 0.7 if no melt occurs and 0.5 during melt. Cumulative snowfall exceeding 5 mm refreshes α_s to 0.85. F_s follows the parameterization given by Yang et al. (1997) such that

$$F_s = \tanh \left(\frac{S_d}{\chi} \right), \tag{4}$$

where χ is an adjustable parameter determining the width of the snow cover depletion curve. Following Verseghy (1991), snow density increases with time such that

$$\rho(t + \Delta t) = \rho_{\max} + (\rho(t) - \rho_{\max}) \exp(-\Delta t/3.6 \times 10^5) \tag{5}$$

3

where $\rho_{\max}$ is the maximum snow density (300 kg m^{-3}). During snowfall, the density of the snowpack is updated such that

$$\rho(t + \Delta t) = \frac{\rho_{\text{fresh}} S_f + \rho(t) SWE}{SWE + S_f} \tag{6}$$

where S_f is snowfall, SWE is snow water equivalent and ρ_{fresh} is fresh snow density (assumed to be 100 kg m^{-3}). SWE is increased by snowfall and decreased by snowmelt.

The exposed vegetation fraction is defined here as the projected exposed plant area, A_{proj}, per area of ground, A. The projected area is

$$A_{\text{proj}} = \sum_{i=1}^{n} (2 r_i x_i) f \tag{7}$$

where n is the number of primary branches, the terms in the bracket are the cumulative products of the diameter and projected horizontal length of the branches that are explicitly modelled and f is a factor introduced to represent the area of secondary branches and marcescent leaves which increase the snow interception area but are not explicitly modelled. Providing that the snow-free vegetation fraction, F_{v0}, and the structure of the primary branches of the shrub are known, f can be calculated as

$$f = F_{v0} \frac{A}{\sum_{i=1}^{n} (2 r_i x_i)}. \tag{8}$$

A is assumed to be a square with the branch with the largest projected x taken as half of the length of its sides. When snow-free, x in Equation 7 is given by

$$x = L \sin \theta_0, \tag{9}$$

where L is branch length and θ_0 is unbent branch angle to the vertical. When there is snow on the ground but branches are unbent,

$$x = L \sin \theta_0 - S_d \tan \theta_0. \tag{10}$$

2.2   Biomechanical branch bending model

The biomechanical model was built by engineering analogy with the elastic theory ("the Elastica") for the large deformation of cantilevers columns. Similar methods were used by Niklas and O'Rourke (1987) for a model of chive bending and by Schmidt and Pomeroy (1990) for a model of conifer branch bending which used the elastic theory of the bending of cantilever beams.

Referring to Figure 1, the curvature of a branch bending under an applied load can be expressed as $d\theta/ds$, where θ is the angle between the branch and the vertical and s is length along the branch. For an untapered branch of radius r with a load M applied at its tip, curvature is related to bending moment by

$$\frac{d\theta}{ds} = \frac{Mg}{EI} x, \tag{11}$$

where g is the gravitational acceleration, E is the Young's (or elastic) modulus and

$$I = \pi r^4 / 4 \tag{12}$$

is the second moment of area about the axis of bending. This equation indicates that the curvature of the branch is not only related to the load on the branch but also inversely proportional to the flexural rigidity,

which is a product of the shape of the branch (I) and its material properties (E). Although a branch will typically taper towards its tip and be loaded by snow distributed along its length, a more complex and computationally expensive numerical solution would be required to account for radii and snow loads varying along the length of branches. These two assumptions partly compensate each other, as explained in Section 4.3.

Taking the derivative of Equation 11 with respect to s and using $dx/ds = \sin\theta$ gives

$$\frac{d^2\theta}{ds^2} = -k^2 \sin\theta, \tag{13}$$

which Timoschenko and Gere (1961) recognised as the pendulum equation with

$$k = (Mg/EI)^{1/2}. \tag{14}$$

The first integral of Equation 13, with boundary conditions of no curvature and deflection angle ω at the tip of the branch, is

$$\frac{d\theta}{ds} = k[2(\cos\theta - \cos\omega)]^{1/2}. \tag{15}$$

Integrating again gives

$$\int_{\theta_0}^{\omega} \frac{d\theta}{k[2(\cos\theta - \cos\omega)]^{1/2}} = L. \tag{16}$$

Introducing

$$p = \sin\frac{\omega}{2} \tag{17}$$

and ϕ such that

$$\sin\phi = p^{-1} \sin\frac{\theta}{2} \tag{18}$$

to change variables gives

$$kL = \int_{\phi_0}^{\pi/2} \frac{d\phi}{(1 - p^2 \sin^2\phi)^{1/2}} = F(p, \pi/2) - F(p, \phi_0) \tag{19}$$

where F is the incomplete elliptic integral of the first kind. Following Aristizábal-Ochoa (2004), horizontal and vertical coordinates at points on the branch are given by the parametric curve

$$x(\phi) = \frac{2p}{k}(\cos\phi_0 - \cos\phi) \tag{20}$$

and

$$z(\phi) = \frac{1}{k}[2E(p, \phi) - 2E(p, \phi_0) - F(p, \phi) + F(p, \phi_0)] \tag{21}$$

for $\phi_0 \leq \phi \leq \pi/2$, where $E(p, \phi)$ is the incomplete elliptic integral of the second kind. Points on the branch are exposed if $z(\phi) > S_d$ or buried if $S_d > z(\phi)$. The horizontal distance between the two points at which $z(\phi)$ is equal to the snow depth for a partly buried branch is used to determine the horizontal projected area used in Equation 7.

Branch spring up is assumed to occur when the height of the tip of the branch exceeds snow depth. Although Pomeroy et al. (2006) suggested that shrub spring up is a mechanical process which is a function of snow depth and snow grain bond weakening rate, the simple spring up parametrization used here was chosen over a more complex one because of the lack of empirical data on this relationship.

2.3 Relationship between SBM and the parameter b

The aim of the model is to improve the representation of albedo over shrub-tundra and, as such, one of the objectives of the model is to help define the b parameter in Equation 1. Here, we propose

$$b = z_{max}/h_c, \tag{22}$$

where z_{max} is the highest point of the branch, which is calculated by the shrub bending model with Equation 21.

3 Description of sites and data

3.1 Sites

The model is evaluated against albedo measured at two sites:

- The 8 km^2 Granger Basin (GB), situated 15 km south of Whitehorse at 60°35'N, 135°11'W in the sub-alpine ecozone of the larger Wolf Creek Research Basin. The basin ranges in elevation from 1295 to 1555 m a.s.l. and is characteristic of shrub-tundra landscapes, with birch on the slopes and willows that are mostly found in the riparian zones at the valley bottom. The model is tested against observations from a willow site described by Bewley et al. (2010).

- The Trail Valley Creek (TVC) research basin tall shrub site, situated at 68°45'N, 133°30'W, approximately 55 km north east of Inuvik, NWT, Canada. TTS (TVC Tall Shrub) is representative of a large patch of tall shrubs (> 125 cm) that cover approximately 2 km^2, composed mainly of green alder and diamond leaf willow. The shrubs do not constitute a closed canopy even when fully emerged. Full descriptions of TVC are provided in Marsh et al. (2008), Marsh et al. (2010) and Endrizzi and Marsh (2010).

3.2 Driving, input and evaluation data

The model is driven by snowfall, snowmelt, air temperature and snow depth and evaluated against albedo measurements. Other factors, such as wetness of snow and wind, which are known to affect interception efficiency and snow load on conifer branches (Schmidt and Gluns, 1991; Hedstrom and Pomeroy, 1998; Pomeroy et al., 2006), are ignored here because their effect on shrub bending is poorly understood; adding these processes would increase the complexity, but not necessarily the accuracy, of the model.

At both sites, air temperature, snow depth and incoming and outgoing short wave radiation were measured by meteorological stations set above the vegetation cover (Figure 2). At TTS, meteorological data are available for the snow seasons 2004-2005 and 2006-2007, hereafter referred to as Years 1 and 2. Solar radiation was sampled every 60 seconds with a Kipp and Zonen CNR1 net radiometer at 5.56 m height and averaged half-hourly. At GB, shortwave radiation was sampled every 60 seconds by a pair of upwards and downwards pointing Kipp and Zonen CM21 pyranometers at 2.89 m and averaged half-hourly for the snow

seasons of 2006-2007, 2007-2008 and 2008-2009 (Years 1, 2 and 3 hereafter). Snow depth was measured with Campbell SR50 ultrasonic ranging sensors at both sites.

Harsh winter conditions caused logistical constraints in accessing meteorological stations which were left unattended for up to 3 months at GB and for the whole winter at TTS. Malfunctions, caused by ice and snow sitting on the upward-facing pyranometers and/or by blowing snow interfering with the reading of the downward facing pyranometers and the ultrasonic depth gauges, sometimes led to poor quality data. In order to address this issue, albedo values were rejected if the outgoing shortwave radiation exceeded a nominal threshold of 85% of the incoming radiation. Daily averages were calculated for days with more than three valid measurements

Snowfall was not recorded at either site, so snowfall data from the nearest Environment Canada (EC) meteorological stations were used (Environment Canada - National Climate Data and Information Archive, 2012). At GB, snowfall data were obtained from Whitehorse International Airport (WIA), which is situated 19 km from the site and 590 m lower in elevation. A correction factor (1.29) calculated by Matt MacDonald (personal communication) from data compiled for MacDonald et al. (2009) was used to adjust snowfall for GB, where precipitation can be up to 40% greater than at WIA (Pomeroy et al., 1999). The nearest EC meteorological station to TVC is 55 km away at Inuvik. The snow depth from the EC data was found to be approximately half that recorded at the site. This may be caused by differences in precipitation but also by the trapping of blowing snow by the shrubs at TTS. As a consequence, the EC data were used to provide the timing of the snowfall events but a correction factor (2.2 in Year 1 and 1.3 in Year 2), calculated by comparing snow depth at Inuvik and at TTS, was applied to the amount of snowfall. Precipitation recorded as rain at the EC stations was assumed to have fallen as snow at the sites if their air temperatures were below $0°$. This difference in the nature of the precipitation was confirmed by observed snow depths increasing at the sites but remaining zero at the EC stations. Snowmelt was calculated from snow depth measurements as

$$M_s = (S_{d(t-\Delta t)} - S_{d(t)})\rho \tag{23}$$

where ρ is snow density, taken to be 300 kg m^{-3} during snowmelt.

3.3 Shrub structure parameters

Table 2 lists the parameters used in the model. Snow-free vegetation fractions were obtained from LiDAR measurements at TTS and from an aerial photograph at GB (Bewley et al., 2007). The parameter χ in Equation 4 was fitted to measured snow cover depletion curves reported by Bewley et al. (2010) at GB and Marsh et al. (2010) at TTS. Ground and vegetation albedos were set to measured snow-free albedos. Ranges of canopy heights, used to calculate branch lengths, and branch radii were measured at GB during field campaigns in Spring 2008 and 2009. At TTS, canopy height range was determined from LiDAR measurements made in July 2004 (Marsh et al., 2010). Branch radius was measured at the base of the branches at TTS and both at the base and breast height (1.30 m) at GB. Tapering of branches with height causes branch radius at breast height, which is the value needed in the model, to be smaller than at base. As branch radii at base were similar at both sites, the same range of values measured at breast height at GB was used for TTS. The maximum angle to the vertical of branches measured at GB was 19°, but this near-vertical

7

geometry was found to be unlike the shrubs at either site, suggesting that measurements had been biased towards the taller, straighter branches. A nominal value of $\theta_0 = 1.22$ radians (70°) was selected to provide a more realistic shrub-like shape. The number of primary branches per shrub was not measured at either site; the value used in the model ($n = 20$) was taken from a description given by Sturm et al. (2005a) of a tall shrub site dominated by *Salix pulchra*, which is also found at GB and TTS. Lengths, radii and angles for each branch in the model were selected at random from uniform distributions across the prescribed ranges.

4 Evaluation of model performance

Figure 3 shows a shrub modelled at TTS at different stages of bending. Figure 3 only shows the part of the branch that is explicitly modelled, *i.e.* there is no representation of the foliage, implicit in the model in f. The shrub prior to any load being applied is shown in Figure 3a. Panels 3b-c show changes in the shape of the shrub throughout the season. Branches bend at different rates because of their individual lengths, radii and initial inclinations. When the shrub is bent but not fully buried, the tip and base of the branch are progressively buried but the middle of the branch still protrudes above the snowpack (Figure 3-b).

4.1 Model evaluation against measured albedo

Figures 4 and 5 show five-day moving averages of modelled and measured albedos at TTS and GB. Two runs with simpler F_v parameterizations were performed for comparison at both sites: one is a modified version of SBM (bury-only) in which shrubs get buried but the branches do not bend (*i.e.* Equations 11 to 21 are not used), and the other has a fixed $F_v = F_{v0}$ (*i.e.* Equations 2 to 6 only). Although there are large gaps in observations because of instrument malfunctions and the small number of daytime hours during winter, the models were run throughout each winter. Quantitative assessments of model performance are given by root mean square errors in Table 3. Average albedo values are shown in Table 4.

4.1.1 Trail Valley Creek

At TTS, simulations of albedo are significantly closer to albedo measurements with SBM than with the fixed-F_v and bury-only models. Many of the albedo measurements during snow accumulation in Year 2 had to be rejected due to snow on the upward facing radiometer, but results for Year 1 suggest that SBM offers considerable improvement compared to the other two models during the first month of the accumulation period. Although the maximum h_c is 1.85 m, Figure 3 shows that the shrub is fully bent and buried when S_d = 0.43 m, resulting in a difference in albedo at that time between the SBM and the bury-only parametrization of 0.29 (0.74 and 0.45 respectively). The albedo data and the model suggest that shrubs became buried in the two specific years studied here, even though Marsh et al. (2010) report that shrubs are not buried every year at TTS.

4.1.2 Granger Basin

SBM does not perform as well at GB as at TTS, and rmse and albedo values in Tables 3 and 4 show that the bury-only model is consistently closer to observations. Although some shrubs near the meteorological

8

station were observed to be bent, it is clear from Figure 2-a that many shrubs within the field of view of the downward-facing pyranometer were erect. SBM consistently overestimates albedo and, although many of the modelled branches remain exposed, this shows that the model bends branches too much compared to the GB observations. SBM is closer to observations than the bury-only model between days 188 and 234 in Year 1, suggesting that some bending could have occurred late in the season. Otherwise, the good fit between the bury-only model and measurements shows that the parameters used give a good overall representation of the shrub structure without bending. Some of the processes that could affect albedo but are omitted in SBM are discussed in Section 4.3, and a discussion of further developments needed in the model is included in Section 5.

4.1.3 Parametrization of exposed vegetation fraction

The parametrization of F_v given by Equation 1 (subsequently referred to as the "b model") was tested by calculating b from SBM results at each timestep using Equation 22 and then using the average value for each site in Equations 1 and 2 to simulate albedo. Average b values and rms errors for albedo simulations are shown in Table 5.

At both sites, the rmse values of the SBM and of the b model show that the latter leads to lower rmse values than the former for 3 out of 5 years, suggesting that the SBM can be used to calculate the parameter proposed by Sturm et al. (2005a). At TTS, there are no noticeable differences between the SBM and the b model. The structural branch parameters lead to the branches behaving uniformly and thus a single parameter is representative of the whole shrub unlike during the accumulation at GB where somes branches bend and spring up while other remain either erect or bent. As a consequence, although the bury-only model is still closer to observations, the b model presents a slight improvement compared to the full SBM because it removes the noise of individual outlying branches on α and F_v during accumulation.

To investigate year-to-year variability within sites, b was also calculated from SBM separately for each year and calibrated to minimize rms errors against observations. At TTS, the calculated and calibrated b values and corresponding rms errors for the b model are close. On the other hand, the full SBM performs poorly at GB and the calibrated b model gives lower rms errors with a b value almost double that calculated from SBM.

4.2 Sensitivity to parameters

Sensitivity of the modelled vegetation fraction and albedo to four site-specific parameters used in the model (snow-free exposed vegetation fraction, Young's modulus, number of branches per shrub and initial branch angle) is presented in Figures 6 and 7. Additional SBM runs were performed with parameter values increased or decreased one at a time; 20% changes in parameters relative to the base runs were used in all cases except for elasticity at TTS, for which the lowest and highest values (1.69 - 3.59×10^9 N m^{-2}) reported by Brüchert et al. (2003) for cold region alders were used because they exceed a $\pm 20\%$ range. Elasticity values were swapped between the sites in another two runs.

The model is more sensitive to parameter variations at GB than at TTS because not all of the modelled branches become buried at GB and changes that increase or decrease the number of buried branches can have

larger effects on F_v and α. There is less scatter at TTS because branches bend more easily and the behaviour of the branches is more uniform, i.e. all of them become buried in snow (Figure 3-c), and the changes in vegetation fraction between runs that do occur have little effect on the albedo. The only exception to this is the run performed with the much higher value of E from GB, for which less bending occurs and the albedo is considerably decreased. This sensitivity shows that the model should only be used where information on the mechanical properties of the shrub species to be modelled are known, and lacking this information could cause large errors.

At both sites, F_v initially increases as snow load increases because the branches are bent outwards as well as downwards (see the x for the erect and bent branch in Figure 1). This only occurs when snow is very shallow and little of the shrub is buried. Field measurements may provide information on the extent to which this process occurs in reality rather than being a model artefact.

4.3   Potential sources of error in the biomechanical model

There have been few detailed field studies focusing on the processes modelled in SBM. More experimental data are needed to gain a better understanding of the timescales over which bending occurs, the spatial distribution of bent shrubs and the influence of weather conditions. This lack of information forces the model to try and represent shrub bending processes as simply as possible but the model might benefit from a greater level of complexity when further information becomes available. Gaps in knowledge remaining in this field mean that the following simplifications were required:

- The elastic modulus was not measured at either site. At GB, the mean value given by Johnson (1987) for *Salix glauca*, one of the species of willow found in GB, was used. At TVC, the average of values given by Brüchert et al. (2003) for different *Alnus* species (green and common alder) found in cold regions was used. E was taken as a constant parameter even though it is known to be affected by (a) temperature (Schmidt and Pomeroy, 1990; Lundström et al., 2008), (b) water availability (Niklas and O'Rourke, 1987) and (c) the direction of measurements to the grain (Niklas, 1992).

- SBM only explicitly models primary branches. Coupling SBM to a structural biological model would provide a more realistic shrub structure but would introduce complications that were not deemed necessary. The purpose of SBM is to ascertain the relationship between the vegetation fraction (F_v) and snow depth in order to parametrize the exposed vegetation fraction, *not* to model the behaviour of individual branches under the weight of snow, which is nonetheless a means to the end. The parameter f was instead introduced to implicitly simulate foliage surrounding primary branches.

- Shrub branches were modelled as untapered rods. However, tapering causes the bending of a loaded branch to increase towards its tip. The same effect is achieved by applying the load at the tip of the branch, which was done in the model to avoid the complexity of having loads distributed along branches.

- Plasticity or non-recoverable deformations are not modelled, meaning that branches return to their pre-load position and shape after they spring up. As the standard deformation in biological materials is approximately 0.1% (Niklas, 1992), it was not considered significant enough to include in the model.

10

- Spring up in SBM is solely a function of snow depth. Relating snow strength to the forces that have to be resisted by snow to prevent a branch from springing up is essential to improve the spring up parameterization.

5 Discussion and Conclusions

Changes in albedo are expected to offset increases in carbon uptake provided by shrub expansion in the Arctic (Fischlin et al., 2007). Predicting the effects of shrub expansion therefore requires models to be able to reproduce albedo over shrubs accurately. The results in Section 4.1.1 showed that omitting the bending and burying of shrubs could lead to average albedo being underestimated by as much as 29%. Such errors in models predicting changes in energy budget at high latitudes would lead to overestimation of the effect of shrubification on climate warming.

This study proposed the first biomechanical shrub bending model for use in calculating shrub-tundra albedo and found it to perform well at one of the two sites tested. However, the performance of the model at GB stresses that further developments are needed, most of which require a more thorough understanding of the mechanical bending processes. Adding further complexity to the parameterisation without first gaining a better understanding of the processes involved in bending could add to model uncertainties rather than improve accuracy. Therefore, some questions remain to be answered: How is elasticity affected by air temperature? Does wind and / or drifting snow affect bending? How quickly do shrubs bend and what are the unloading processes? Until such knowledge is gained and the model is tested in catchment-scale studies with known shrub structural parameters, the model cannot confidently provide the parameter b required in the calculation of vegetation fractions for use in large-scale land surface models.

As mentioned in the Introduction, measurements of shrub bending are difficult to obtain because of the random nature of bending (shrubs do not bend every year) and the destructive nature of measurements (*e.g.* information on wood elasticity can only be obtained by cutting, or at least moving, branches). As a consequence, proxy data are used to determine the extent of shrub bending (exposed vegetation fraction, albedo). Using albedo as a measure to evaluate model performance causes further uncertainties as to the source of the error. Whereas both the bury-only model and the calibrated b model perform well at GB in Years 2 and 3, they do not manage to capture albedo variability as well in Year 1. It is currently unclear whether this is due to deficencies in the calculation of F_v or other variables that have a large influence over alebdo in Equation 2, e.g. F_s and α_s.

An additional complication is that, as there have been no previous models describing the mechanical bending processes, it has been unclear which data need to be collected to improve our knowledge. Understanding process-based mechanisms is often incremental and model developments can be very helpful in suggesting which parameters need to be defined by field measurements. The model presented in this paper is one such model. Combining the few, mostly qualitative, observations available with a biomechanical model derived from engineering theory has provided a first approximation of bending mechanisms. As importantly, the model has allowed the identification of measurements that are needed in order to improve the model and our understanding of the occurrence of shrub bending. In order to obtain this first bending model, many assumptions have been needed and future research should concentrate on replacing these assumptions with

solid quantitative, rather than qualitative, process-based data. Nevertheless, the performance of the model and the remaining uncertainties allow a reassessment of the hypotheses advanced by previous studies and listed in Section 1:

1. Relationships between snow wetness, temperature and bending were not tested.

2. Although the necessity of high winds was not tested directly, bending occurred in SBM even though it is not driven by wind speed. This shows that the weight of the snow alone can cause bending.

3. Bending of some of the branches at TTS occured within a single daily timestep, confirming that bending can occur during a single snowfall event.

4. Equations 13 to 19 show that stem diameter and species are two of the three structural factors controlling bending. The biomechanical model shows that the "species factor" mentioned in Sturm et al. (2005b) is the Young's modulus, which is species dependent. The third factor, omitted in the Sturm et al. (2005b), is branch length.

5. Non-systematic burial is supported by results at GB which suggest that there was more burial of shrubs in Year 1 than Year 3.

6. Bending occurred in the two years the model was tested at TTS, where the shrubs are willows and alder, but little bending occurred for the willows at GB. Although the model would need to be tested at more sites, the results for TTS and GB do not currently agree with this hypothesis.

7. Relationships between snow metamorphism, branch elasticity and spring up were not tested.

By simulating the geometrical properties of bent shrub branches and using them to calculate the compression factor b, the model proposed here aims to enhance our understanding of the physical processes in bending of shrub branches by using well understood processes, namely the bending of a cantilever, in order to inform poorly understood canopy-scale changes in exposed vegetation. We conclude that:

1. The model provides a tool with which to study shrub bending under intercepted snow loads and to identify critical research needs in snow-shrub interaction studies. Given measurable biomechanical information on shrubs, the model is able to calculate the shape and exposed part of each branch.

2. Given estimates of shrub structure parameters (height, branch radius, number of branches per shrub and modulus of elasticity) which are easy to measure, the model performs well at a shrub-tundra site where shrubs become fully bent and buried in winter but overestimates bending at a site where many branches stay erect.

3. The full SBM can be used to calculate the compression factor required by a less computationally expensive model.

4. Notwithstanding the encouraging performance of the model, further improvements are required. Of critical importance are field measurements of the exposed vegetation fraction which would allow the model output to be directly evaluated against field data rather than rely on a proxy (albedo) which could hide weaknesses in other areas of the model.

12

An automatic camera taking regular images of the bending and unbending of shrubs at a site with good meteorological instrumentation could provide useful information. A camera was, in fact, installed at GB in 2008 for this study, but it was stolen before the images could be retrieved.

Although SBM was used here to calculate the albedo of shrub-tundra, the model could be applied to improve other challenging aspects of modelling shrub-tundra landscapes. For example, information from the model can be used to describe the changing roughness of the surface as branches bend, which is important when determining aerodynamic resistances for modelling turbulent heat exchanges and wind transport of snow.

6   Acknowledgements

References

Aristizábal-Ochoa, J. (2004). Large deflection stability of slender beam-columns with semirigid connections: Elastica approach. *Journal of Engineering Mechanics*, 130:274–282.

Beismann, H., Wilhelmi, H., Bailleres, H., Spatz, H., Bogenrieder, A., and Speck, T. (2000). Brittleness of twig bases in the genus *Salix*: fracture mechanics and ecological relevance. *Journal of Experimental Botany*, 51:617–633.

Bewley, D., Essery, R., Pomeroy, J., and Ménard, C. (2010). Measurements and modelling of snowmelt and turbulent heat fluxes over shrub tundra. *Hydrology and Earth System Sciences*, 14:1331–1340.

Bewley, D., Pomeroy, J., and Essery, R. (2007). Solar radiation transfer through a subarctic shrub canopy. *Arctic, Antarctic and Alpine Research*, 39:365–374.

Brüchert, F., Gallenmüller, F., Bogenrieder, A., and Speck, T. (2003). Stem mechanics functional anatomy and ecology of *Alnus viridis* and *Alnus glutinosa*. *Feddes Repertorium*, 114:181–197.

Chapin III, F., Sturm, M., Serreze, M., and 18 others (2005). Role of land-surface changes in arctic summer warming. *Science*, 310:657–660.

Endrizzi, S. and Marsh, P. (2010). Observations and modeling of turbulent fluxes during melt at the shrub-tundra transition zone 1: point scale variations. *Hydrology Research*, 41:471–491.

Environment Canada - National Climate Data and Information Archive (2012). `http://climate.weatheroffice.gc.ca/climateData/canada_e.html`. Accessed on 23/3/2012.

Fischlin, A., Midgley, G., Price, J., Leemans, R., Gopal, B., Turley, C., Rounsevell, M., Dube, O., Tarazona, J., and Velichko, A. (2007). 2007: Ecosystems, their properties, goods, and services. In Parry, M., Canziani, O., Palutikof, J., van der Linden, P., and Hanson, C., editors, *Climate Change 2007: Impacts, Adaptation and Vulnerability. Contribution of Working Group II to the Fourth Assessment Report of the Intergovernmental Panel on Climate Change*. Cambridge University Press, Cambridge.

Hedstrom, N. and Pomeroy, J. (1998). Measurements and modelling of snow interception in the boreal forest. *Hydrological Processes*, 12:1611–1625.

Johnson, E. (1987). The relative importance of snow avalanche disturbance and thinning on canopy plant populations. *Ecology*, 68:43–53.

Liston, G. and Hiemstra, C. (2011). Representing grass- and shrub-snow-atmosphere interactions in climate system models. *Journal of Climate*, 24:2061–2079.

Loranty, M., Goetz, S., and Beck, P. (2011). Tundra vegetation effects on pan-arctic albedo. *Environment Research Letters*, 6:doi:10.1088/1748–9326/6/2/024014.

Lundström, T., Jonas, T., and Volkwein, A. (2008). Analysing the mechanical performance and growth adaptation of Norway spruce using non-linear finite-element model and experimental data. *Journal of Experimental Botany*, 59:2513–2528.

MacDonald, M., Pomeroy, J., and Pietroniro, A. (2009). Parameterizing redistribution and sublimation of blowing snow for hydrological models: tests in a mountainous subarctic catchment. *Hydrological Processes*, 23:2570–2583.

Marsh, P., Bartlett, P., Mackay, M., Pohl, S., and Lantz, T. (2010). Snowmelt energetics at a shrub tundra site in the Western Canadian Arctic. *Hydrological Processes*, 24:DOI: 10.1002/hyp.7786.

Marsh, P., Pomeroy, J., Quinton, W., Onclin, C., Russell, M., Neumann, N., Pietroniro, A., Davison, B., and McCartney, S. (2008). Snowmelt processes and runoff at the Arctic treeline: Ten years of MAGS Research. In Woo, M-K, editor, *Cold Region Atmospheric and Hydrologic Studies, The Mackenzie GEWEX Experience. Volume 2: Hydrologic Processes*, pages 97–124. Springer, Berlin.

Niklas, K. (1992). *Plant Biomechanics*. The University of Chicago Press, Chicago.

Niklas, K. and O'Rourke, T. (1987). Flexural rigidity of chive and its response to water potential. *American Journal of Botany*, 74:1033–1044.

Pomeroy, J., Bewley, D., Essery, R., Hedstrom, N., Link, T., Granger, R., Sicart, J.-E., Ellis, C., and Janowicz (2006). Shrub tundra snowmelt. *Hydrological Processes*, 20:923–941.

Pomeroy, J., Hedstrom, N., and Parviainen, J. (1999). The snow mass balance of wolf creek: effects of snow, sublimation and redistribution. In Pomeroy, J. and Granger, R., editors, *Wolf Creek Research Basin: Hydrology, Ecology, Environment*. Environment Canada.

Schmidt, R. and Gluns, D. (1991). Snowfall interception on branches of three conifers species. *Canadian Journal of Forest Research*, 21:1262–1269.

Schmidt, R. and Pomeroy, J. (1990). Bending of a conifer branch at subfreezing temperatures: implications for snow interception. *Canadian Journal of Forest Research*, 20:1250–1253.

Sturm, M., Douglas, T., Racine, C., and Liston, G. (2005a). Changing snow and shrub conditions affect albedo with global implications. *Journal of Geophysical Research*, 110:doi:10.1029/2005JG000013.

Sturm, M., Schimel, J., Michaelson, G., Welker, J. M., Oberbauer, S. F., Liston, G. E., Fahnestock, J., and Romanovsky, V. E. (2005b). Winter biological processes could help convert arctic tundra to shrubland. *Bioscience*, 55:17–26.

Timoschenko, S. and Gere, J. (1961). *Theory of elastic stability*. McGraw-Hill, New York.

Verseghy, D. (1991). CLASS - A Canadian land surface scheme for GCMS. I. Soil model. *International Journal of Climatology*, 11:111–133.

Yang, Z.-L., Dickinson, R. E., Robock, A., and Vinnikov, K. (1997). On validation of the snow sub-model of the biosphere-atmosphere transfer scheme with Russian snow cover and meteorological observational data. *Journal of Climate*, 10:353–373.

Definition	Symbol	Unit
Albedo	α	-
Ground albedo	α_g	-
Snow albedo	α_s	-
Shrub albedo	α_v	-
Angle of a segment of branch to the vertical	ϕ	rad
Snow density	ρ	kg m^{-3}
Fresh snow density	ρ_{fresh}	kg m^{-3}
Angle between branch and the vertical	θ	rad
Branch angle before bending	θ_0	rad
Snow cover depletion parameter	χ	m
Deflection angle at tip of branch	ω	rad
Ground area	A	m^2
Exposed shrub area	A_{proj}	m^2
Compression factor	b	-
Young's or elastic modulus	E	N m^{-2}
Foliage factor	f	-
Complete elliptic integral of the first kind	$F(p)$	-
Snow fraction	F_s	-
Vegetation fraction	F_v	-
Snow-free vegetation fraction	F_{v0}	-
Gravitational acceleration	g	m s^{-2}
Canopy height	h_c	m
Second moment of area	I	m^4
$(Mg/EI)^{1/2}$	k	m^{-1}
Branch length	L	m
Load applied on branch	M	kg
Number of primary branches	n	-
$\sin \omega/2$	p	rad
Branch radius	r	m
Distance along branch	s	m
Snow depth	S_d	m
Snowfall	S_f	kg m^{-2}
Snow water equivalent	SWE	kg m^{-2}
Horizontal coordinates of branch elements	x	m
Vertical coordinates of branch elements	z	m

Table 1: List of symbols.

	Granger Basin	Trail Valley Creek
α_g, α_v	0.11	0.14
θ_0 (rad)	1.22	1.22
χ (m)	0.17	0.20
E (N m^{-2})	4.197×10^{10} (Johnson, 1987)	2.69×10^9 (Beismann et al., 2000)
F_{v0}	0.71 (Bewley et al., 2007)	0.75 (LiDAR, Marsh et al., 2010)
h_c (m)	1.44 to 2.15	1.21 to 1.85 (LiDAR, Marsh et al., 2010)
n	20 (Sturm et al., 2005)	20 (Sturm et al., 2005)
r (m)	0.007 to 0.1	0.007 to 0.1

Table 2: Shrub structure parameter values used in the Shrub Bending Model.

	GB			TTS	
	Year 1	Year 2	Year 3	Year 1	Year 2
	$n = 167$	$n = 195$	$n = 150$	$n = 128$	$n = 73$
SBM	0.16	0.17	0.20	0.07	0.10
Bury-only	0.13	0.08	0.06	0.22	0.28
Fixed-F_v	0.22	0.16	0.18	0.31	0.38
b	0.13	0.13	0.14	0.08	0.09

Table 3: Root mean square errors between observations and each model configuration. n is the number of observed values used for evaluation each year.

	GB			TTS	
	Year 1	Year 2	Year 3	Year 1	Year 2
Observations	*0.37*	*0.35*	*0.37*	*0.58*	*0.60*
SBM	0.53	0.51	0.53	0.64	0.62
Bury-only	0.43	0.40	0.43	0.43	0.40
Fixed-F_v	0.22	0.22	0.23	0.33	0.31

Table 4: Mean albedos values.

	b		rmse	
	Modelled	Calibrated	Modelled	Calibrated
TTS all years	0.24	0.26	0.08	0.07
TTS Year 1	0.33	0.29	0.06	0.05
TTS Year 2	0.16	0.15	0.09	0.09
GB all years	0.44	0.84	0.16	0.09
GB Year 1	0.42	0.69	0.14	0.10
GB Year 2	0.47	0.85	0.13	0.07
GB Year 3	0.45	0.98	0.17	0.05

Table 5: Values of the compression factor b obtained from SBM and calibrated to albedo measurements, and rms errors in albedo simulations using those values.
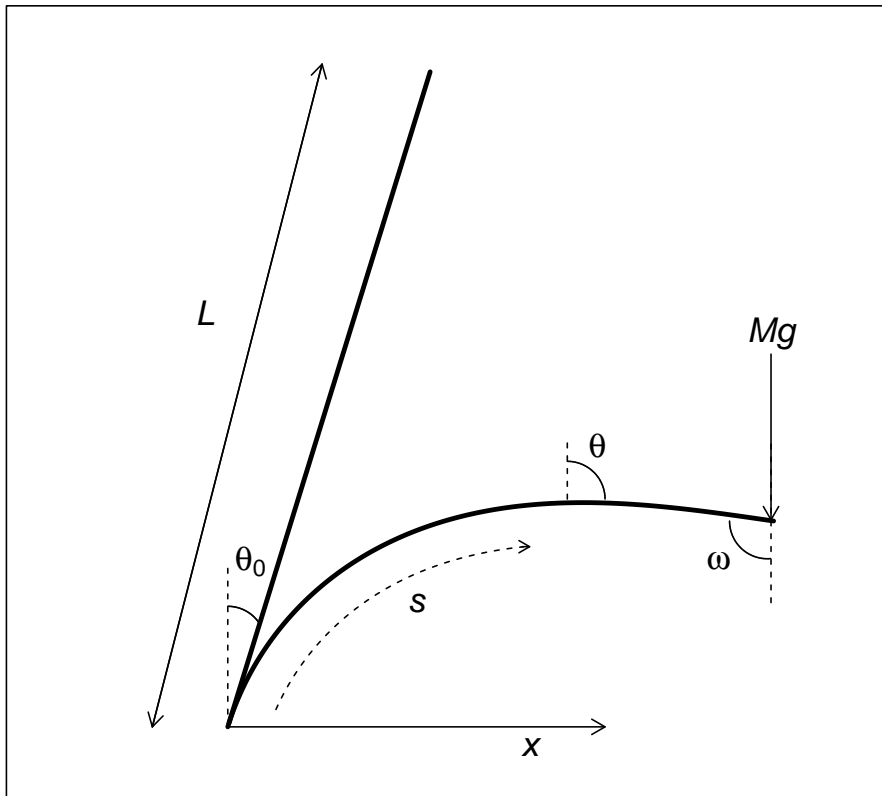
Figure 1: Side view of a branch before and after bending under an applied load.

Figure 2: Meteorological stations at (a) Granger Basin on 15 February 2008, with inset of the snow depth gauge, and (b) the Trail Valley Creek Tall Shrub site on 23 May 2008.
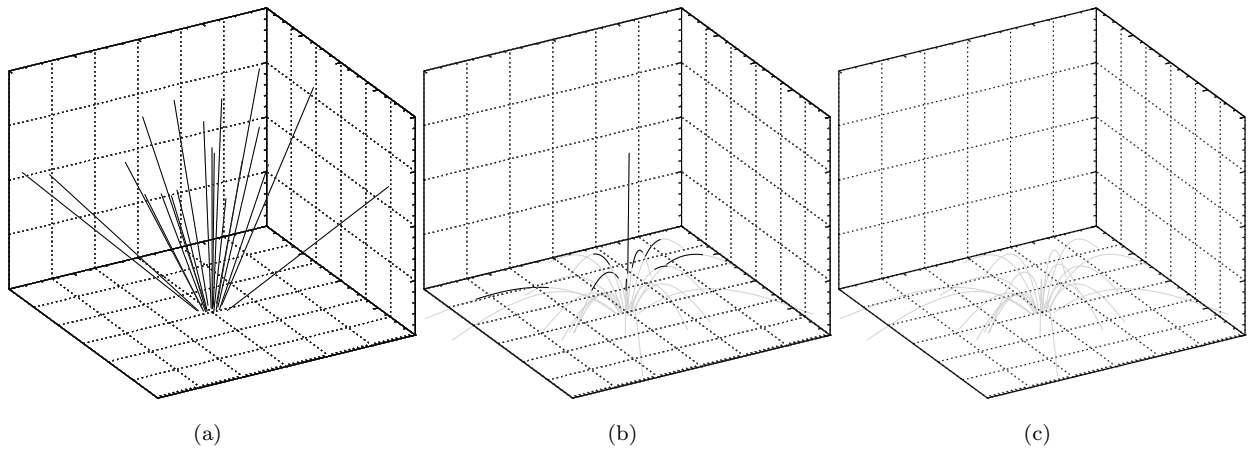
Figure 3: Shape of the shrub at TTS during Year 1 (a) when snow-free, (b) during bending and burying on 3 November($S_d = 0.33$ m) and (c) on the first day the shrub is fully buried (19 January, $S_d = 0.43$ m). The exposed part of the shrub is in black and the buried part is grey.
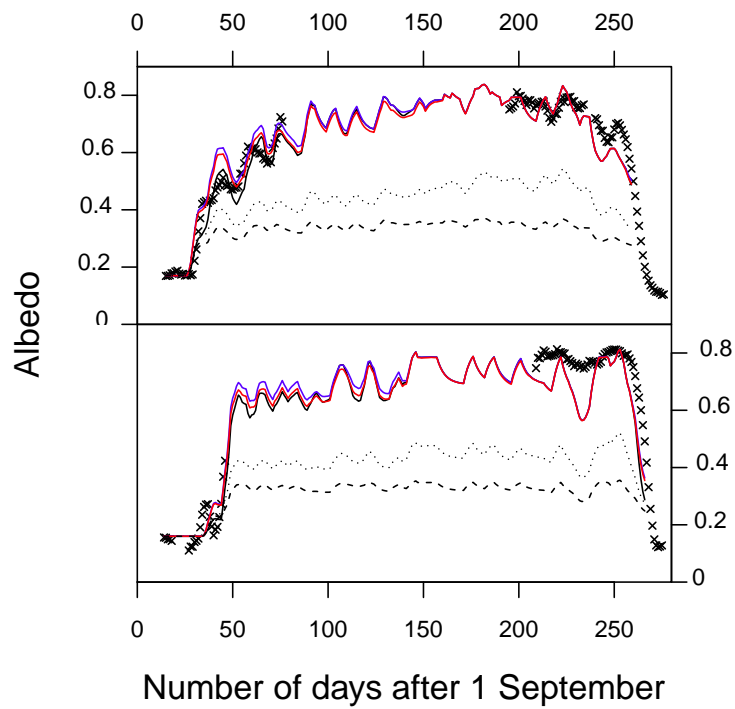
Figure 4: Measured albedo (crosses) and albedo modelled with SBM (solid black line), the bury-only parametrization (dotted line), the fixed-F_v parametrization (dashed line), the b model (blue line) calculated with the SBM and the calibrated b (red) for Years 1 (top) and 2 (bottom) at Trail Valley Creek.
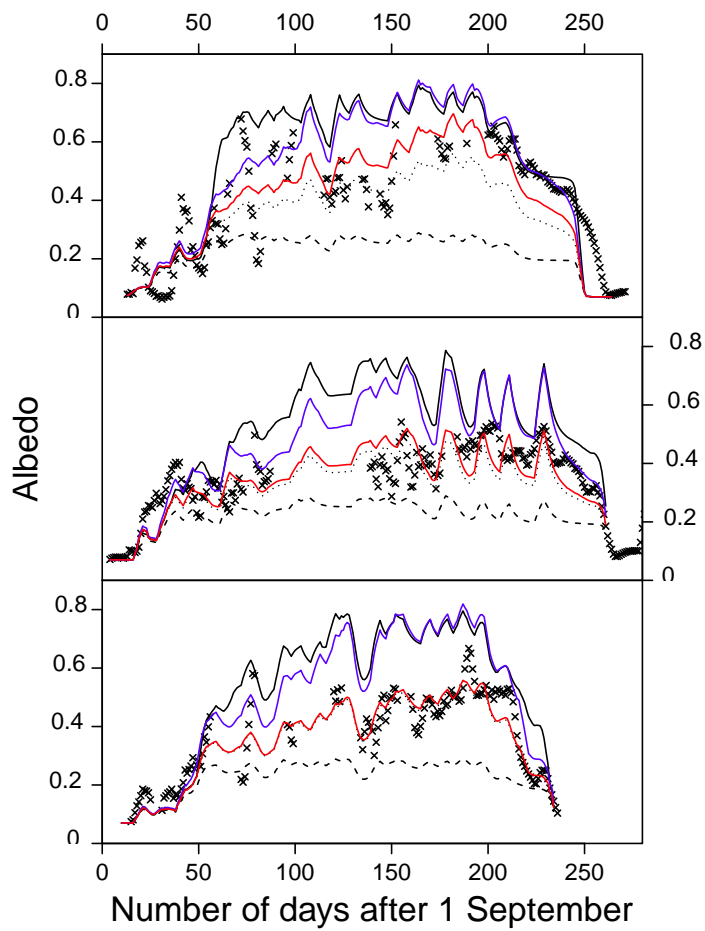
Figure 5: As Figure 4, but for Years 1 (top) to 3 (bottom) at Granger Basin.
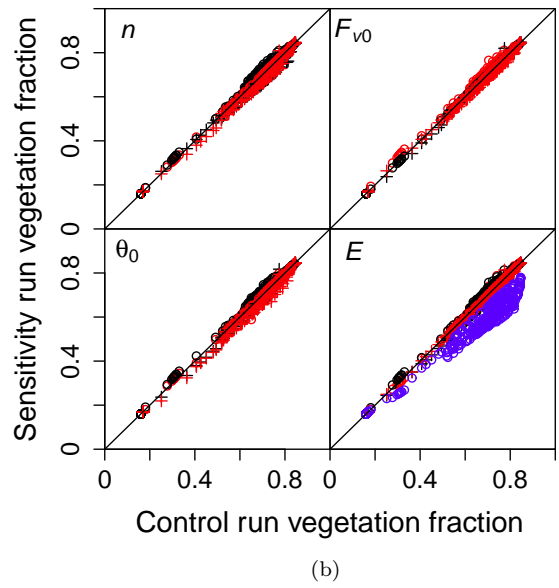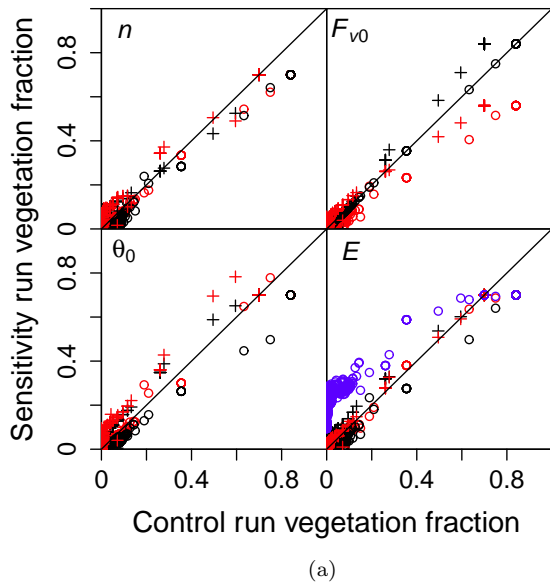
Figure 6: Sensitivity of (a) vegetation fraction and (b) albedo at TTS shown as scatterplots of the sensitivity runs against control runs. The parameter varied is shown in the upper left corner of each plot. Red is for runs with reduced parameter values and black for increased values. Circles are for Year 1 and crosses for Year 2. Blue is the run with the elastic modulus from GB.
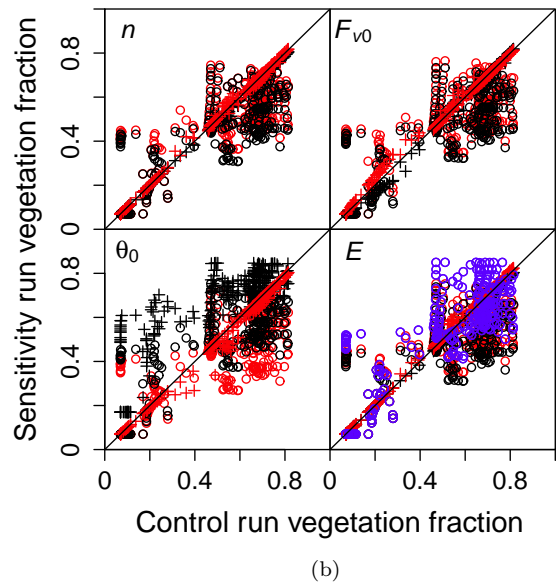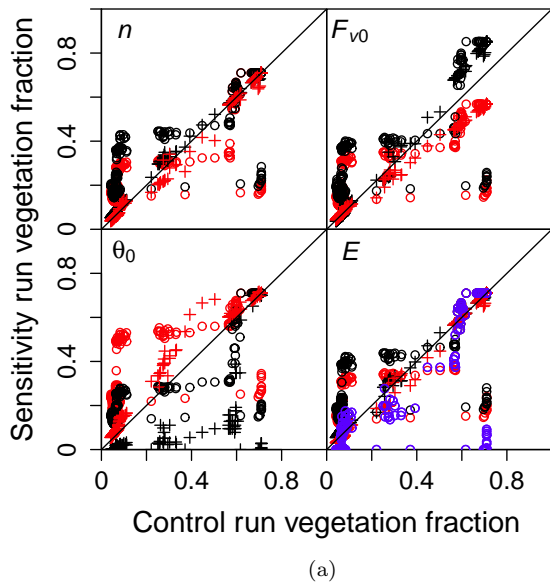

Figure 7: As Figure 6, but for GB in Year 1 and 2. Blue is the run with the elastic modulus from TTS.